JOURNAL OF MATERIALS SCIENCE 31 (1996) 1311–1317

Magnetic and electrical properties of Al^{3+}-substituted $MgFe_2O_4$

K. B. MODI, H. H. JOSHI, R. G. KULKARNI
Department of Physics, Saurashtra University, Rajkot 360005, India

The structural, magnetic and electrical properties of the Al^{3+}-substituted disordered spinel system $Mg(Fe_{2-x}Al_x)O_4$ have been investigated by X-ray diffraction, magnetization, a.c. susceptibility and electrical resistivity measurements. The cation distribution derived from the X-ray diffractometry data was found to agree very well with the cation distribution obtained through Mössbauer spectroscopy. The variation of saturation magnetization per formula unit as a function of aluminium context, x, has been satisfactorily explained on the basis of Neel's collinear spin model and the slight discrepancy between the observed and calculated n_B values can be explained in terms of a random canting model. The Néel temperatures calculated theoretically by applying molecular field theory agreed well with the experimentally determined values from thermal variation of susceptibility and electrical resistivity. An unusual metal-like thermo-electric behaviour was found for the compositions with $x \geqslant 0.3$ which was attributed to the decrease in the Fe–Fe separation distance arising from aluminium substitution.

1. Introduction

A knowledge of cation distribution and spin alignment is essential to understand the magnetic properties of spinel ferrites. The interesting physical and chemical properties of ferro-spinels arise from their ability to distribute the cations among the available tetrahedral and octahedral sites [1]. In addition, the variation in preparation conditions can cause large changes in some extrinsic properties. The majority of ferrites are highly resistive materials making them more suitable for high-frequency and low-loss applications.

Magnesium ferrite ($MgFe_2O_4$) with diamagnetic substitution for Mg^{2+} and Fe^{3+} ions, has attracted the attention of a number of research workers who attempted to explain the exchange interactions in the spinel lattice on the basis of only one type of magnetic ions (namely Fe^{3+} distributed between the octahedral, B, and tetrahedral, A, sites) being involved in this system which makes the analysis reliable. The structural and magnetic characteristics of magnesium ferrite with a non-magnetic substitution such as Zn^{2+} [2], Cd^{2+} [3], Ti^{4+} [4] have been investigated by means of ^{57}Fe Mössbauer spectroscopy.

Magnesium ferrite aluminates $Mg(Fe_{2-x}Al_x)O_4$ belong to a large class of compounds having the general formula $A^{2+}B^{3+}O_4$ and crystallize in a spinel structure. The metal ions are situated in oxygen tetrahedra and octahedra. According to the literature [5, 6], $MgFe_2O_4$ ($x = 0.0$) is a partially inverse spinel and it can be considered as a collinear ferrimagnet whose degree of inversion depends on the thermal history of the sample. $MgAl_2O_4$ ($x = 2.0$) is a normal spinel with 15% Al^{3+} ions occupying tetrahedral (A) sites [7]. The basic magnetic properties of these materials depend upon the distribution of Fe^{3+} ions among B and A sites of the spinel lattice. The advantage of the mixed spinel considered here is that all interactions are well-defined near-neighbour antiferromagnetic with $|J_{AB}| \gg |J_{BB}| \gg |J_{AA}|$, where J_{AB}, J_{BB} and J_{AA} are exchange integrals. Thus, the antiferromagnetic A–B superexchange interactions is the main cause of the cooperative behaviour of the magnetic dipole moments known as ferrimagnetism, which is observed in magnesium ferrite aluminates below their Néel temperatures. For almost inverse $MgFe_2O_4$ the measured value of the saturation magnetic moment per molecule is 1.0 μ_B which is solely determined by the magnetic moment of the Fe^{3+} ion (5 μ_B). In $Mg(Fe_{2-x}Al_x)O_4$, the value of that moment is altered by substitution of non-magnetic Al^{3+} ions.

No systematic study of the concentration dependence of magnetic and electrical properties of $Mg(Fe_{2-x}Al_x)O_4$ have been reported in the literature, except infrared spectroscopy [8], dielectric constant [9], and Mössbauer investigation [10] at $x = 0.2$, 0.4 and 0.7. Hence an attempt has been made to investigate the effect of Al^{3+} substitution on the magnetic and electrical properties of $MgFe_2O_4$ by means of magnetization, susceptibility and electrical resistivity measurements. The compositional dependence of saturation moments is explained on the basis of collinear and randomly canted spin arrangements. The variation of Néel temperature as a result of Al^{3+} substitution is explained on the basis of a random distribution of incomplete superexchange interactions. The effects on the conduction mechanisms of varying aluminium concentration and temperature are discussed in detail.

0022–2461

2. Experimental procedure

The samples of the spinel solid solution series $Mg(Fe_{2-x}Al_x)O_4$ for $x = 0.0$–1.4 with steps of $x = 0.1$, were prepared by the standard ceramic method. The appropriate quantities of MgO, Al_2O_3 and Fe_2O_3 (all 99.9% pure and supplied by E. Merck) were thoroughly mixed, pelletized and sintered at 950 °C for 12 h. The X-ray patterns for all the samples were recorded at room temperature with a Philips (PM 9220) diffractometer using FeK_α radiation. The experimental details regarding the Mössbauer spectrometer were given elsewhere [11].

The magnetic measurements of the samples were carried out using a high-field hysteresis loop technique [12]. The a.c. susceptibility of powdered samples within the temperature range 77–800 K were performed using double-coil apparatus [13] operating at 263 Hz and an r.m.s. field of 0.5 Oe. The samples for electrical measurements were in the form of discs 10 mm in diameter and 3 mm thick. The two faces of each disc sample were polished by rubbing with zero grade emery paper. Thereafter samples were washed in dilute HCl and acetone. Graphite was rubbed on both flat faces of the samples on which aluminium foils were also kept for good electrical contacts. The porosity of all the samples calculated by using bulk and X-ray density was within 10%–12%. The resistance of a pellet was measured by the two-terminal pressure-contact method using a BPL-made meg-ohm meter. Thermal variation of resistivity was obtained by placing the sample holder containing a pellet in a horizontal electric furnace.

3. Results and discussion

The X-ray powder diffractograms showed the presence of cubic spinel phase with no extra lines corresponding to any other phase. The X-ray lines were found to be sharp, which makes the detection of any impurity phase easy. The values of lattice constant a were determined with an accuracy of $\pm$ 0.0002 nm. The variation of lattice constant with aluminium concentration, x, is shown in Fig. 1. The lattice constant gradually decreases with increasing x. Usually in a solid solution of spinels within the miscibility range, a linear change in the lattice constant with the concentration of the components is observed [14]. The linear decrease in lattice constant is due to the replacement of larger Fe^{3+} ions (0.064 nm) by the smaller Al^{3+} ions (0.051 nm) in the system $Mg(Fe_{2-x}Al_x)O_4$. The X-ray density decreases with aluminium concentration, x (Fig. 1), because the decrease in mass overtakes the decrease in volume of the unit cell.

To determine the cation distribution of the compounds, X-ray diffraction intensity calculations were carried out and compared with the observed ones. The intensity ratios of the planes $I(220)/I(440)$ and $I(422)/I(400)$ are considered to be sensitive to the cation distribution and their relationship with composition is represented in Fig. 2. The atomic scattering powers of various ions were taken from the literature [15]. The intensity ratios have been calculated taking into consideration the possible combinations of

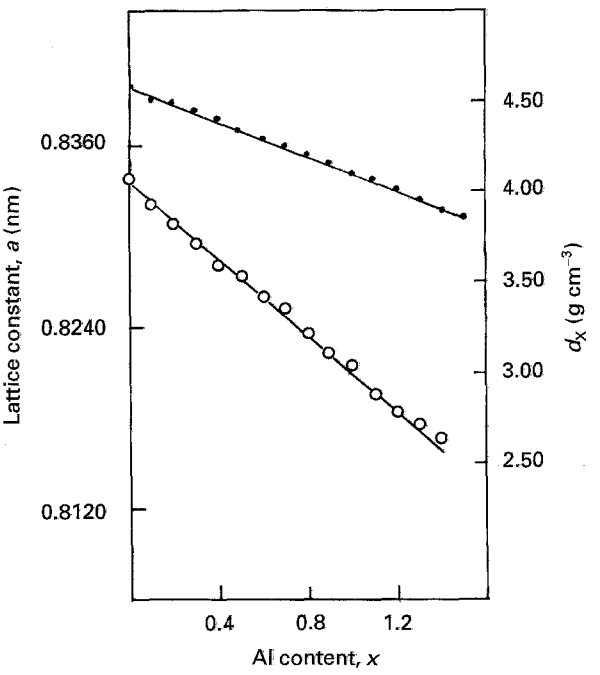

Figure 1 Variation of (○) lattice constant, a, and (●) X-ray density, d_X, with aluminium concentration, x.

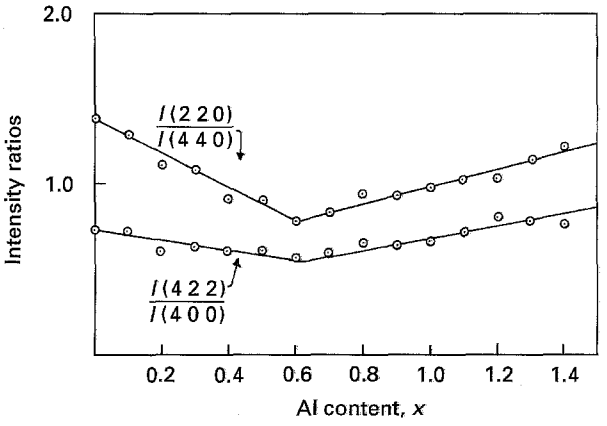

Figure 2 The relationship between the intensity ratios of planes $I(220)/I(440)$ and $I(422)/I(400)$ and composition, x, for $Mg(Fe_{2-x}Al_x)O_4$.

cations, and were compared with the observed intensity ratios. The values of intensity ratios decrease linearly with increasing Al^{3+} substitution, show a minimum at $x \sim 0.6$ and then gradually increase on further dilution. This behaviour is attributable to the variation in the Fe^{3+} ion concentration at the tetrahedral site which is induced by Al^{3+} substitution in the unit cell.

We have estimated the cation distributions through Mössbauer spectral intensity calculations by considering the integrated areas under the Lorentzians corresponding to tetrahedral, A, and octhedral, B, sites which were taken as proportional to the amount of Fe^{3+} ions on these sites. Typical computer-fitted Mössbauer spectra for $x = 0.2$ and 0.4 at 298 K are displayed in Fig. 3. The variation of B-site and A-site Mössbauer spectral intensity ratio, I_B/I_A, as a function of aluminium substitution, x, is depicted in Fig. 4 which agrees well with the variation of cation

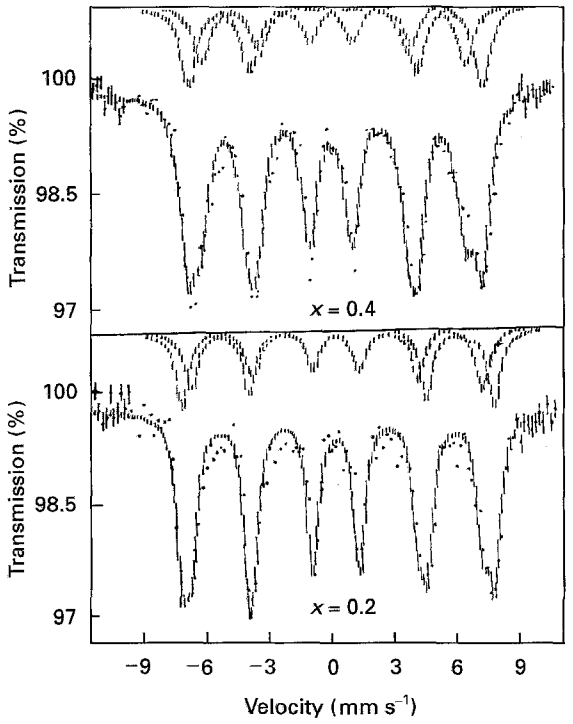

Figure 3 Mössbauer spectrum of $x = 0.2$ and 0.4 at 298 K. (——) The result of least squares computer fit.

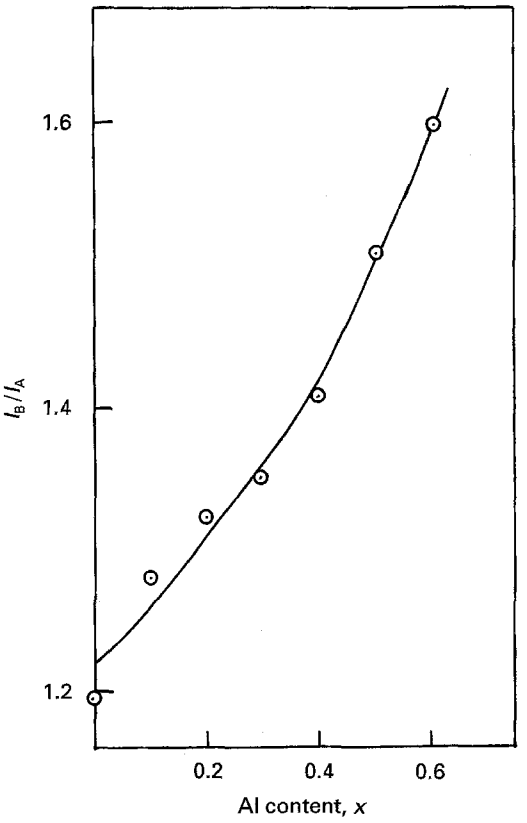

Figure 4 Mössbauer integrated intensity ratio: (○) octahedral to tetrahedral sites = I_B/I_A, and (——) cation distribution parameter $\delta = Fe_B^{3+}/Fe_A^{3+}$.

distribution parameter, $\delta = Fe_B^{3+}/Fe_A^{3+}$ with x. The cation distribution has been derived from X-ray diffraction and Mössbauer results and the distribution parameter $\delta = (Fe_B^{3+}/Fe_A^{3+})$ for each composition is given in Table I. The detailed Mössbauer study on this system has been reported elsewhere [11].

Because magnesium aluminate is a near-normal spinel, 85% of the Al^{3+} ions occupy B sites in the spinel system [7]. The Fe^{3+} concentration of A and B sites decreases simultaneously with increasing aluminium content, x, in the ratio of 3:2 for $x = 0.0$–0.6 and about 3:7 for $x = 0.7$–1.4, respectively. The cationic distributions obtained for $Mg(Fe_{2-x}Al_x)O_4$ are represented as

$$x = 0.0\text{–}0.6$$

$$(Fe^{3+}_{0.9-0.6x}Al^{3+}_{0.15x}Mg^{2+}_{0.1+0.45x})^{A}$$

$$[Mg^{2+}_{0.9-0.45x}Al^{3+}_{0.85x}Fe^{3+}_{1.1-0.4x}]^{B}O^{2-}_{4}$$

$$x = 0.6\text{–}1.2,\ y = 0.0\text{–}0.8 \qquad (1)$$

$$(Fe^{3+}_{0.54-0.3y}Al^{3+}_{0.09+0.15y}Mg^{2+}_{0.37+0.15y})^{A}$$

$$[Mg^{2+}_{0.63-0.15y}Al^{3+}_{0.51+0.85y}Fe^{3+}_{0.86-0.7y}]^{B}O^{2-}_{4} \qquad (2)$$

The saturation magnetization, σ_s, and the magneton number, n_B (saturation magnetization per formula unit in Bohr magneton) at 77 K obtained from magnetization data for the samples with $x = 0.0$–1.2, are listed in Table I. Figure 5 shows the variation of n_B with x for $x = 0.0$–1.2. It is seen that the value of

TABLE I Saturation magnetization, σ_s, magneton number, n_B, cation distribution parameter ($\delta = Fe_B^{3+}/F_A^{3+}$), and canting angle $\langle\alpha_\beta^c\rangle$ for the $Mg(Fe_{2-x}Al_x)O_4$ system

x	Magnetization (77 K)		Calculated $n_B(\mu_B)$	δ	δ [10]	Canting angle $\langle\alpha_B\langle exp\rangle\rangle$ (deg)
	σ_B(e.m.u. g^{-1})	$n_B(\mu_B)$				
0.0	28	1.05	1.0	1.220		–
0.1	31	1.09	1.1	1.262		3.52
0.2	32	1.10	1.2	1.308	1.14	11.37
0.3	33	1.13	1.3	1.361		15.14
0.4	40	1.35	1.4	1.424	1.22	8.37
0.5	44	1.45	1.5	1.500		8.54
0.6	47	1.55	1.6	1.593		8.75
0.7	42	1.36	1.4	1.549	1.32	8.16
0.8	37	1.17	1.2	1.500		7.40
0.9	31	0.98	1.0	1.444		6.36
1.0	26	0.79	0.8	1.381		4.76
1.1	21	0.58	0.6	–		–
1.2	15	0.32	0.4	–		–

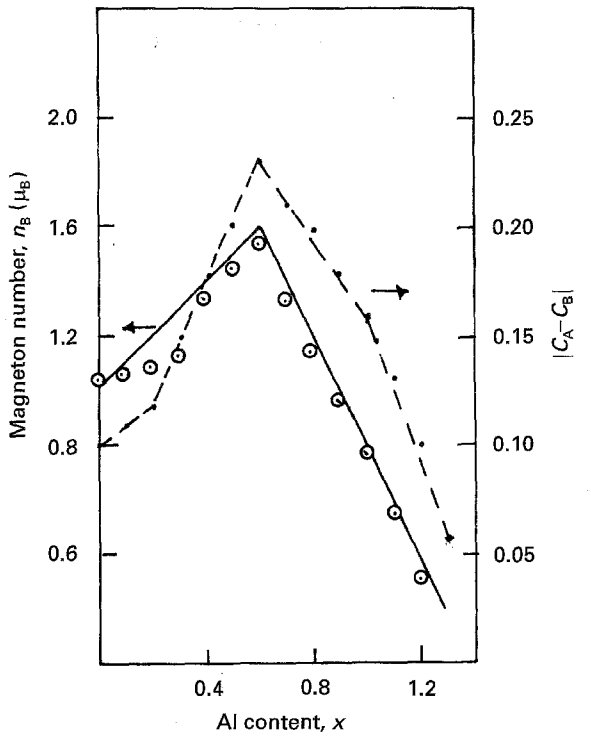

Figure 5 (○) Variation of saturation magnetic moment per formula unit n_B at 77 K, and (- - -) the difference between the fraction of iron concentration on A and B sites. $|C_A - C_B|$, with aluminium content, x. (———) Néel's model.

n_B gradually increases with increasing aluminium concentration, x, attains a maximum at $x \sim 0.6$ and decreases almost linearly with further increase in x from $x = 0.6$–1.2.

It is evident from Fig. 5 that the difference between the fraction of magnetic ion (Fe^{3+}) on A-site and on B-site, $|C_A - C_B|$ is 0.1 for a collinear ferrite $MgFe_2O_4$ ($x = 0.0$) and it increases linearly with aluminium concentration, x, and becomes 0.23 for $x = 0.6$ then decreases linearly on further dilution to 0.055 for the sample with $x = 1.0$. This suggests that the overall predominance of intersublattice (A–B) superexchange interaction should remain almost constant over intrasublattice (B–B) exchange interaction in spite of non-magnetic Al^{3+} substitution. This allows Néel's collinear spin model to be applied to explain the variation of n_B with aluminium, x, for $Mg(Fe_{2-x}Al_x)O_4$ system.

According to Néel's two sublattice model of ferrimagnetism, Néel's magnetic moment per formula unit in μ_B, n_B^N, is expressed as

$$n_B^N = M_B(x) - M_A(x) \quad (3)$$

where M_B and M_A are the B and A sub-lattice magnetic moments in μ_B. The calculated values of n_B^N using the cation distributions (Equations 1 and 2) and Néel's Equation 3 for $x = 0.0$–1.2, shown as a solid line in Fig. 5, agree well with the experimentally found n_B values, except for the compositions with $x = 0.1$, 0.2 and 0.3.

For a chemically disordered system such as $Mg(Fe_{2-x}Al_x)O_4$ it is quite possible that the canting is not uniform but instead is locally dependent upon the statistical distribution of non-magnetic neighbouring ions. Therefore, the increase in Al^{3+} substitution leads to the localized non-collinearity of the ferrimagnetic phase. In this region effective moments are created with ferrimagnetic structure by local canting around the magnetic imperfections introduced by aluminium substitution. Therefore, the slight disagreement between the observed and calculated n_B value (as per Néel's model) can be explained in terms of a random canting model [16]. According to the model the nearest neighbours of a B-site can be considered to be canted with an average angle $\langle\alpha_\beta\rangle$ due to A-site substitution which, in the average nearest neighbour approximation is estimated to be

$$\cos\langle\alpha_\beta\rangle \approx (M_A/M_B)(J_{AB}/J_{BB}) \quad (4)$$

The total magnetization per unit formula is related to canting angle, $\langle\alpha_\beta^C\rangle$, by

$$n_B^C = M_B \cos\langle\alpha_\beta\rangle - M_A \quad (5)$$

where M_A and M_B are sub-lattice magnetizations of A and B sites to be determined from the cation distributions (1) and (2), J_{AB} and J_{BB} are exchange integrals. The experimental value of the canting angles, $\langle\alpha_\beta^C(\text{exp})\rangle$have been obtained from Equation 5 using measured n_B values (Table I), and are given in Table I. It is evident from Table I that the $\langle\alpha_\beta^C(\text{exp})\rangle$ values fluctuate arbitrarily with increasing x, indicating random canting of B-site moments.

Although we agree with Sundarajan *et al.* [10] that small canting exists for $x = 0.1$–0.4 and is assumed to be random, unlike A-site canting assumed later [10], our cation distributions (Equations 1 and 2) do not agree with the values previously determined [10] by applying a magnetic field externally on Mössbauer spectra for $x = 0.2$, 0.4 and 0.7. In addition, magnetic moments, n_B, have been calculated with A-site canting using the cation distribution given by Sundarajan *et al.* [10], and n_B values for $x = 0.2$, 0.4 and 0.7, are found, respectively, to be 0.82 μ_B, 0.94 μ_B and 0.88 μ_B. These calculated n_B values again do not agree with the experimentally measured values (Table I). The observed differences in the cation distribution and n_B values for $x = 0.2$, 0.4 and 0.7 between the present work and previous work [10] may be due to different preparation conditions and cooling rates employed in the synthesis of the samples.

Typical plots of relative low-field (0.5 Oe) a.c. susceptibility, χ/χ_{RT} (RT = room temperature), against temperature, T, for $x = 0.2$, 0.4, 0.6 and 0.8 are shown in Fig. 6, which exhibit normal ferrimagnetic behaviour. The Néel temperatures, T_N, determined from a.c. susceptibility measurements are listed in Table II. It is evident from Table II that there is a sharp decrease in Néel temperature for small additions of aluminium, which is due to the decreasing Fe^{3+}–O^{2-}–Fe^{3+} superexchange linkages resulting from replacement of Fe^{3+} by Al^{3+} in the spinel lattice.

The Néel temperatures have also been calculated theoretically for $x = 0.1$–1.0 applying molecular field theory and using the cation distribution found from Mössbauer spectroscopic and X-ray diffraction measurements. The Néel temperature depends upon the active magnetic linkages per magnetic ion per

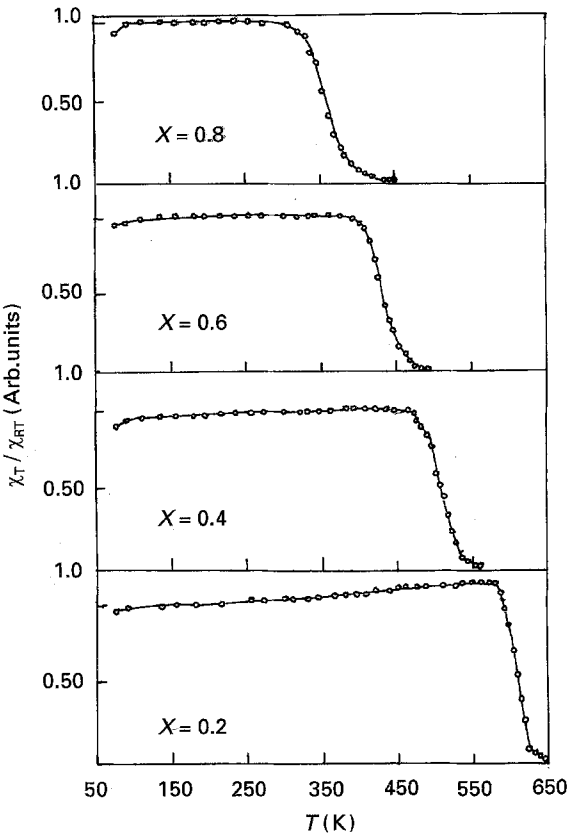

Figure 6 Thermal variation of low-field a.c. susceptibility for $x = 0.2$, 0.4, 0.6 and 0.8.

TABLE II Néel temperature, T_N, and activation energy, E, for the $Mg(Fe_{2-x}Al_x)O_4$ system

x	T_N(K)			E(eV)	
	Susceptibility	Resistivity	Calculated	Para.	Ferri.
0.0	725	715	725	0.550	0.41
0.1	675	663	680	0.921	0.450
0.2	635	635	642	1.258	0.420
0.3	585	560	603	0.738	[a]
0.4	550	—	564	0.929	[a]
0.6	478	—	483	0.920	[a]
0.8	400	—	397	0.712	[a]
0.9	357		356		
1.0	317		315		

[a] Metal-like behaviour.

formula unit [17]. The average number of magnetic interactions, $n(x)$ for a ferrite with non-magnetic substitution, x, is given by

$$n(x) = \frac{1}{N}[f_t f_o (Z_{BA} k_o + Z_{AB} k_t)] \quad (6)$$

where f_t and f_o are the fractions of magnetic ion concentrations with respect to unsubstituted ferrite and k_t and k_o are number of metal ions at tetrahedral and octahedral sites, respectively, Z_{BA} and Z_{AB} denote the A-site nearest neighbours to the B-site, and the B-site nearest neighbours to the A-site, respectively, N is the total number of magnetic ions in a substituted ferrite. Thus, Equation 6 reduces to

$$n(x) = \frac{24}{N}[f_t f_o] \quad (7)$$

The influence of Al^{3+} ion substitution upon Néel temperature of unsubstituted ferrite $MgFe_2O_4$ may be approximated through its effect upon the average number, $n(x)$, of Fe^{3+}–O^{2-}–Fe^{3+} superexchange interactions per magnetic ion (Fe^{3+}) per formula unit. In $MgFe_2O_4$ ($x = 0.0$) there are 24/2 interactions per magnetic ion Fe^{3+} which is denoted by interactions per magnetic ion Fe^{3+} which is denoted by $n\,(x = 0)$. The degree of inversion for unsubstituted $MgFe_2O_4$ ($x = 0.0$), deduced from the Mössbauer spectral intensity ratio, I_B/I_A, is 90% (Fig. 4). The introduction of non-magnetic Al^{3+} into $MgFe_2O_4$ will reduce $n(x = 0)$ which is expressed by using Equations 1 and 7, as

$$n(x) = \frac{24}{2-x}\left[\frac{(1.1-0.4x)}{1.1}\frac{(0.9-0.6x)}{0.9}\right] \quad (8)$$

Therefore, the Néel temperature of Al^{3+}-substituted $MeFe_2O_4$, $T_N(x)$, will vary approximately as $n(x)$, so that it can be related to the Néel temperature of $MgFe_2O_4$, T_N $(x = 0)$, by

$$T_N(x) = \frac{n(x)}{n(x=0)} T_N(x=0)$$

or

$$T_N(x) = \frac{2(1.1-0.4x)(0.9-0.6x)}{(1.1)(0.9)(2-x)} T_N(x=0) \quad (9)$$

The Néel temperatures estimated using Equation 9 for $x \leqslant 0.6$ are in very good agreement with the measured values, and are given in Table II. Similarly the Néel temperatures for the samples with $x \geqslant 0.6$ can be calculated using cation distribution Equation 2 as

$$T_N(y) = \frac{2(0.54-0.3y)(0.86-0.7y)}{(2-y)(0.54)(0.86)} T_N(y=0) \quad (10)$$

where $x = 0.6 + y$; $y = 0.0$–0.8 and $T_N(y = 0)$ is the Néel temperature of a sample with $x = 0.6$. The difference observed between measured and calculated Néel temperature values is due to the random variation of the number of Fe^{3+}–O^{2-}–Fe^{3+} interactions per Fe^{3+} ion as a consequence of the random distribution of Al^{3+} ions in A- and B-sites.

The Seebeck coefficient measurements [18] on magnesium ferrite aluminates, $Mg(Fe_{2-x}Al_x)O_4$ have established that all the samples except those with $x = 0.0$, 0.1 and 0.2 were n-type semiconductors. This indicates that the most probable conduction mechanism is electron hopping between Fe^{2+} and Fe^{3+} ions

$$Fe^{2+} \rightleftharpoons Fe^{3+} + e \quad (11)$$

This process is expected to take place between two adjacent octahedral sites in a spinel lattice.

The compositional dependence of resistivity at room temperature is shown in Fig. 7. The resistivity increases with increase in aluminium concentration, x. This happens because the replacement of Fe^{3+} by Al^{3+} dilutes conduction through the octahedral sites. The incorporation of Al^{3+} ions which do not participate in the conduction process, limits the degree of Fe^{2+}–Fe^{3+} conduction that ocurs. Thus the efficient

method of curtailing the conduction process is the replacement of the effective ions (Fe^{2+}–Fe^{3+}) by less effective ones (Al^{3+}).

The electrical resistivity as a function of temperature for the system $Mg(Fe_{2-x}Al_x)O_4$ in the form of

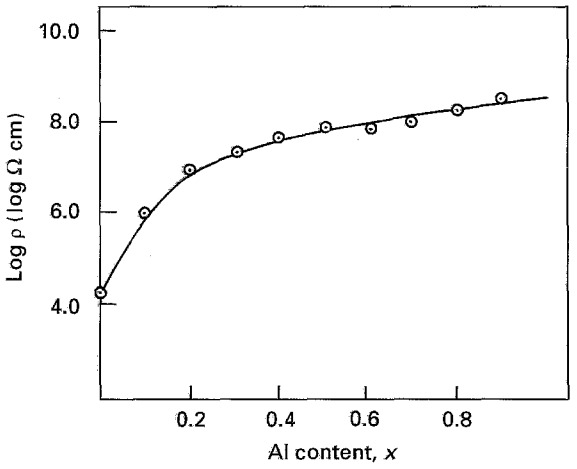

Figure 7 The dependence of electrical resistivity upon aluminium content, x.

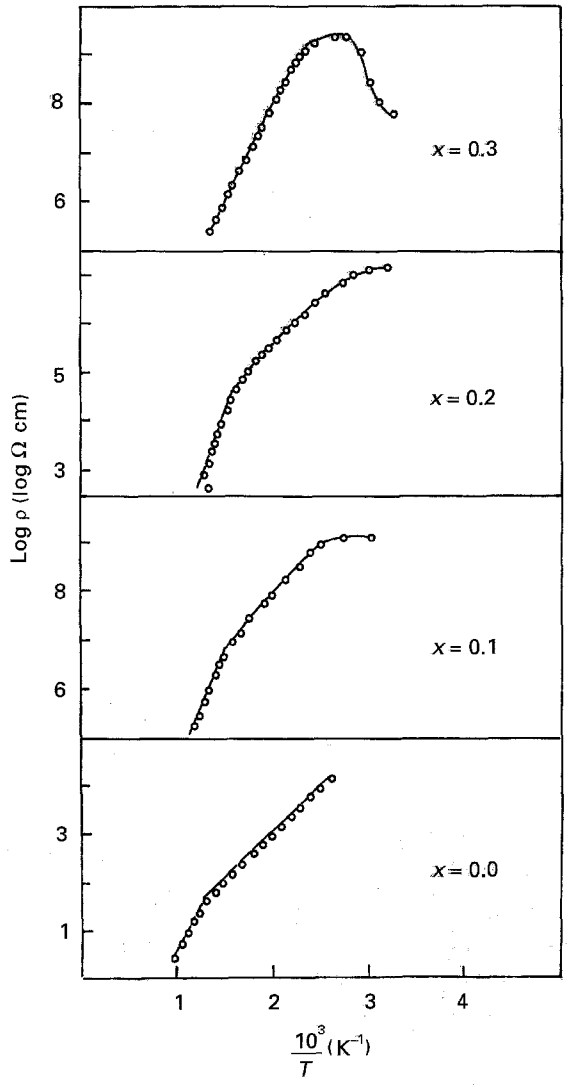

Figure 8 Electrical resistivity versus temperature for $x = 0.0$, 0.1, 0.2, and 0.3.

Arrhenius plots of $\log \rho$ versus $10^3/T$ are shown in Figs 8 and 9 for the compositions with $x = 0.0$, 0.1, 0.2, 0.3, 0.4, 0.6 and 0.8. The temperature dependence of resistivity is given by the Arrhenius equation

$$\rho = \rho_0 \exp[\Delta E/kT] \quad (12)$$

where k is Boltzmann's constant, and ΔE is the activation energy. The activation energy values for conduction are computed from these plots and are listed in Table II. It is seen that (Fig. 8, $x = 0.0$, 0.1, 0.2) the slope of $\log \rho$ versus $10^3/T$ curve changes at the Néel temperature, T_N. The activation energy increases on changing from the ferrimagnetic to the paramagnetic region (Table II). This anomaly strongly supports the influence of magnetic ordering upon the conductivity process in ferrites. The Néel temperatures determined for $x \leqslant 0.2$ from $\log \rho$ versus $10^3/T$ plots are given in Table II. It is not possible to identify the slope change and therefore the Néel temperature point for the samples with $x > 0.3$ because of their unusual thermal characteristics.

Generally, the electrical resistivity of ferrites decreases with increase in temperature. This type of conventional behaviour is observed for the compositions with $x = 0.0$, 0.1 and 0.2 (Fig. 8). It is important to note the differences in the $\log \rho$ versus $10^3/T$ curves (Figs 8 and 9) with increasing x. For the compositions with $x \geqslant 0.3$, the resistivity initially increases with increasing temperature within the temperature range 300–500 K; thereafter it follows the conventional behaviour of decreasing resistivity with increase in temperature. The anomalous electrical behaviour of

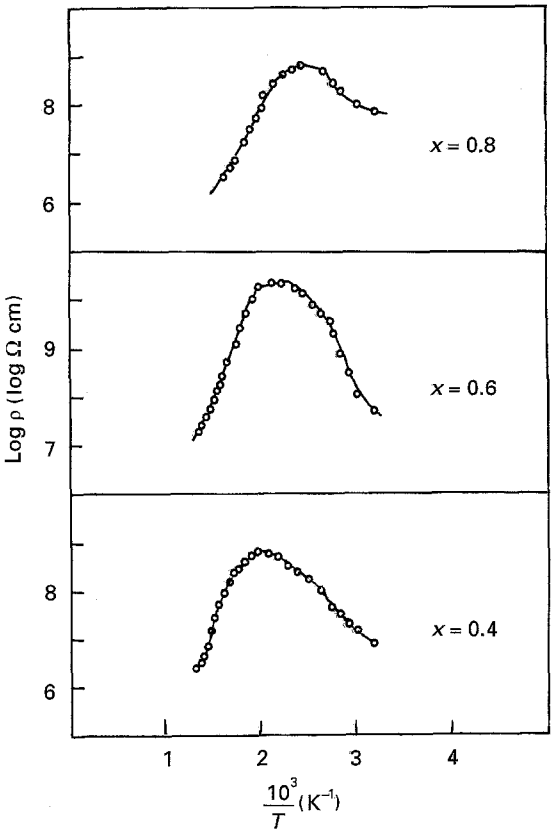

Figure 9 Electrical resistivity versus temperature for $x = 0.4$, 0.6 and 0.8.

d.c. resistivity as a function of temperature for Sn^{4+} and Zn^{2+}-substituted $NiFe_2O_4$ has been explained on the basis of electron hopping and current, due to electrons in the conduction band [19]. The metal-like unusual characteristic observed in the vanadium spinels, LiV_2O_4, has been explained in terms of the distance between two neighbouring B-site vanadium ions [20]. Along the same lines, it may be assumed that the sufficient ($x \geqslant 0.3$) replacement of larger Fe^{3+} (0.064 nm) ions by smaller Al^{3+} (0.051 nm) ions in $Mg(Fe_{2-x}Al_x)O_4$, decreases the B-site Fe–Fe separation distance below a certain critical value where, besides electron-hopping, a nearly band-like conductivity may occur. This is characterized by the metallic conductivity in the temperature range 300–500 K. When the sample temperature is raised above a certain value, the B-site Fe–Fe separation increases above the critical value due to thermal expansion of the unit cell. This hampers the band-like conduction mechanism and again the major conduction mechanism through electron-hopping between two adjacent B-sites becomes dominant. Thus the conventional thermal behaviour observed for a sample temperature greater than 500 K is ascribed to electron hopping mechanism. With Al^{3+} substitution there is no significant variation in the temperature at which maximum resistivity is obtained. The reduction in the lattice constant, a, due to aluminium substitution for the samples with $0.3 \leqslant x \leqslant 0.8$ is 0.0057 nm. This indicates that an almost equal amount of thermal energy may be required to increase the B-site Fe–Fe ion separation distance above a certain critical value.

4. Conclusion

A correlated study of the spinel system $Mg(Fe_{2-x}Al_x)O_4$ clearly shows that the magnetic properties of this system are determined by the distribution of the magnetic ion, Fe^{3+}, among A and B sites. The study also confirms that the Néel temperature is directly proportional to the number of active superexchange linkages per magnetic ion per formula unit. The replacement of the effective larger ions, Fe^{3+}, by less-effective smaller ions, Al^{3+}, brings about the rise in the electrical resistivity and the unusual metal-like thermal behaviour.

Acknowledgements

The authors thank Dr G. K. Bichile, Marathwada University, and Dr G. J. Baldha, Saurashtra University, for fruitful discussions. K. M. thanks Saurashtra University for providing financial support in the form of a Research fellowship.

References

1. G. BLASSE, *Philips Res. Rep. Suppl.* **3** (1964).
2. R. G. KULKARNI, and H. H. JOSHI, *Solid State Commun.* **49** (1985) 1005.
3. R. V. UPADHYAY and R. G. KULKARNI, *ibid.* **48**(8) (1983) 69.
4. R. A. BRAND, H. GEORGES-GILBERT, J. HUBSCH and J. A. HELLER, *J. Phys. F Mater. Phys* **15** (1985) 1987.
5. H. KNOCK and H. DANNHEIM, *Phys. Status Solidi A* **37** (1976) K 135.
6. E. DE GRAVE, C. DAUVE, A. GOVAERT and J. D. SITTER, *Phys. Status Solidi B* **73** (1967) 527.
7. U. SCHMOCAER, H. R. BOESCH and F. WALDNER, *Phys. Lett.* **40A** (1972) 237.
8. K. V. S. BADARINATH, *Phys. Status. Solidi (a)* **K19** (1985) 639.
9. L. G. VAN UITERT, *Proc. IRE* **October** (1956) 1294.
10. M. D. SUNDARAJAN, A. NARAYANASAMY, T. NAGARAJAN, L. HAGGSTRON, C. S. SWAMY and K. V. RAMANUJACHARY, *J. Phys. C Solid State Phys.* **17** (1984) 2453.
11. KUNAL B. MODI, H. H. JOSHI and R. G. KULKARNI, *Solid State Commun.* submitted.
12. C. RADHAKRISHNAMURTY, S. D. LIKHITE and N. P. SASTRY, *Philos. Mag.* **23** (1971) 503.
13. C. RADHAKRISHNAMURTY, S. D. LIKHITE and P. W. SAHASTRABUDHE, *Proc. Ind. Acad. Sci.* **87A** (1978) 245.
14. C. G. WHINFREY, D. W. ECKART, A. TAUBER, *J. Am. Chem. Soc.* **82** (1960) 2695.
15. "International Tables for the determination of Crystal structure", Vol. 3 (Kynoch Press, Birmingham, 1968).
16. A. ROSENCWAIG, *Cand. J. Phys.* **48** (1970) 2857.
17. M. A. GILLEO, *J. Phys. Chem. Solids* **13** (1960) 33.
18. A. P. NIKOLSKII, *Sov. Phys. Solid State* **8** (1966) 960.
19. U. VARSHNEY, R. J. CHURCHILL, R. K. PURI and R. G. MENDORATTA, in "Proceedings of the 5th International Conference on Ferrite", Vol. 1, edited by C. M. Srivastava, Bombay, (1989) p. 255.
20. D. B. ROGERS, J. L. GILSA, T. E. GIER, *Solid State Commun.* **5** (1967) 143.

Received 1 December 1994
and accepted 8 September 1995